# Quantitative modulated excitation Fourier transform infrared spectroscopy

Dieter Baurecht[a] and Urs Peter Fringeli
*Institute of Physical Chemistry, University of Vienna, A-1090 Vienna, Austria*

(Received 3 April 2001; accepted for publication 3 July 2001)

The detection of weak absorption changes induced by an external excitation is often hindered by intense background absorptions as well as by noise. Modulation spectroscopy is an adequate tool to be applied in such a case, provided the system may be periodically stimulated, leading to a periodic reversible or pseudoreversible response. In modulated excitation (ME) Fourier transform infrared spectroscopy the phase sensitive detection (PSD) used for the demodulation of the periodic system response is generally performed during data acquisition, i.e., applied to the intensity of the interferogram. This leads to a number of problems in quantitative analysis and the requirement of optional equipment. In this article, a method is presented to perform an off-line vector PSD of conventional time-resolved spectra after data acquisition. A detailed mathematical analysis of PSD applied to the spectral intensity, the interferogram intensity, and to time-resolved spectra is presented. It is shown, that vector PSD applied to a set of time-resolved spectra is straightforward and avoids any additional mathematical corrections. Furthermore, it will be shown how ME spectroscopy can be used for experimental separation of overlapping bands and a detailed description for the determination of absolute modulation amplitudes and phase lags is given.  [DOI: 10.1063/1.1400152]

## I. INTRODUCTION

The detection of small spectral changes is often hindered by background overlapping. As a consequence, accurate background compensation is a prerequisite for reliable signal detection. The commonly used method to overcome this problem is difference spectroscopy.[1] However, more sophisticated techniques using time dependent stimulation may be applied, as soon as the system under observation responds to the change of an external parameter such as pressure $p$, temperature $T$, concentration $c$, ultraviolet-visible (UV-VIS) light flux $\Phi$, electric potential $\Psi$ a.s.o.

In practice, there are two distinct methods for external stimulation which additionally supply information about kinetic parameters of the reaction: the relaxation technique (parameter jump)[2] and the modulation technique (parameter modulation).[3] The latter can always be applied, when the system responds reversibly or quasireversibly to a periodic external excitation. Consequently, if a modulated absorbance is observed, it has unambiguously to be assigned to those parts of the system that have been affected by modulated excitation (ME). Provided ME has been exerted selectively, the response of the system will consist mainly of modulated absorption bands with the stimulation frequency $\omega$ (fundamental frequency) or multiples of it (harmonics). However, the major part of absorption bands in the stationary spectrum will not be marked by the modulation frequency $\omega$ or higher harmonics. Thus, in the electronic engineer's view all parts which are absorbing light but are not affected by ME will result in a dc spectral response, while ME affected absorbing parts result in an ac response.

Background elimination may now be performed by the separation of the ac and dc parts in the overall signal. It is well known in electronics, that this problem is most efficiently solved by the application of phase sensitive detection (PSD), also referred to as quadrature demodulation.[4] The apparatus and the environment contributions to the overall absorption are generally not affected by ME and therefore are included in the dc response. PSD enables not only the separation of ac and dc components, but also a selective detection of only those signals that exhibit exactly a multiple of the stimulation frequency $\omega$ used in ME. For that purpose PSD is a narrow band technique leading to a dramatic improvement of the signal to noise ratio by the elimination of most background signals from the system.

Moreover, modulation experiments give access to a kinetic analysis of the dynamic processes initiated by ME. If the period of the external stimulation is in the range of relaxation times of the system, both amplitude and phase lag of the response will depend on the modulation frequency $\omega$. With increasing frequency, a decrease of the amplitudes and an increase of phase lags of the fundamental frequency and all harmonics of the system response will result. In case of a sinusoidal stimulation higher order harmonics in the system response indicate a nonlinear signal transfer. Considering, e.g., chemical kinetics, nonlinear responses are typical for all reaction steps differing form first order kinetics. For a review, the reader is referred to Refs. 3 and 5.

Since after PSD, the modulation amplitude of a distinct absorption varies proportionally to the cosine of the difference between the corresponding phase lag $\varphi$ and the operator controlled phase setting $\phi^{\mathrm{PSD}}$, i.e., $\cos(\varphi-\phi^{\mathrm{PSD}})$, the signal intensity varies harmonically as $\phi^{\mathrm{PSD}}$ varies between 0 and $2\pi$. Variation of $\phi^{\mathrm{PSD}}$ in equidistant steps results in a set of so called phase-resolved modulation spectra. In practice,

[a]Author to whom correspondence should be addressed; electronic mail: dieter.baurecht@univie.ac.at

 

phase-resolved modulation spectra are not only the basis for kinetic analysis but may be very useful for the separation of heavily overlapped absorption bands. A prerequisite, however, is that the two overlapping signals result from parts in the stimulated system that exhibit different kinetics, which is manifested by different phase lags with respect to the stimulation. Under this condition the maxima of the corresponding signals appear in different phase-resolved spectra, i.e., at different phase settings $\phi^{\mathrm{PSD}}$. Consequently, the amplitude zero crossings also occur in different spectra which are $\pm 90°$ apart from the corresponding spectra containing the maxima.

This feature of PSD may be most efficient for the separation of a weak signal from an intense overlapping one. In this case, the operator controlled $\phi^{\mathrm{PSD}}$ has to be selected in such a manner that the strong signal vanishes completely, thus enabling the experimental determination of the relevant parameters of the weak band, such as position, half width, and absorbance amplitude $A$. In the case of a chemical system the latter is linearly related to the concentration $c$ of the species by Lambert–Beer's law [Eq. (1)]. As a consequence, the primary signal measured in Fourier transform infrared (FTIR) spectroscopy, the intensity of the interferogram, and the spectral intensity calculated by the Fourier transform will depend exponentially on the concentrations of species affected by ME. This nonlinearity must be taken into account in the interpretation of the system response, as soon as large absorbance amplitudes occur.

Up to the time when digital signal processing (DSP) became fast enough, PSD of modulated signals was performed by analog lock-in amplifiers.[6–9] In a first step analog PSD was replaced by DSP[10] or digital lock-in amplifiers. In current developments DSP circuits of the spectrometers are used to replace external digital signal processing.[11,12] In any case, however, PSD is performed during data collection of the interferogram which may lead to the following problems:

(1) Only the step–scan technique can be used to carry out modulation experiments,[13] which complicates or even prevents low frequency modulation experiments due to long measurement times.

(2) The phase correction needed for the fast Fourier transformation (FFT) of the interferogram becomes more complicated because of the different character of phase-resolved and stationary spectra.

(3) For simultaneous data evaluation at different phase settings $\Phi_{\mathrm{PSD}}$, as well as at higher harmonic responses, additional lock-in amplifiers and data acquisition channels are needed unless new and fast software algorithms are introduced by manufacturers.

(4) The interferogram corresponding to the mean absorbance spectrum has to be measured simultaneously or consecutively with the modulation spectrum to allow quantitative analysis and to evaluate the phase spectrum needed for the phase correction of the modulation interferogram.[14] Additional electronics or software is therefore needed.

(5) Only absorbance modulation amplitudes $\ll 1$ are allowed unless further correction of data is performed[15] when using Lambert–Beer's law for quantitative analysis.

These problems, together with additional costs and complicated nontransparent algorithms in spectrometer specific software, could be the reason why the advantages of modulation spectroscopy were not widely used up to now. In this article, we will report on the principles and the mathematical requirements of a method avoiding the problems just stated.

The only experimental prerequisite is the measurement of time resolved spectra of a periodically stimulated system, which can be done by any data acquisition technique. This enables a wide range of modulation frequencies that are only limited at the low end by the sample stability and at the high end by instrumental electronics.[16,17] Neither analog or digital lock-in amplifiers nor built in DSP are needed because a vector PSD[18] of previously collected time-resolved spectra is performed. Both the mean absorbance spectrum and the phase-resolved modulation spectra of the fundamental frequency and of higher harmonics can be calculated without repetition of experiments. Modulation amplitudes of the response can cover the hole absorbance range without further corrections since Lambert–Beer's law has been taken into account upon data processing.

Finally, we want to emphasize that the method described here for ME-FTIR spectroscopy is more generally applicable to any spectroscopic application that enables time-resolved measurements.

## II. THEORY OF PHASE SENSITIVE DETECTION

A modulated perturbation of the sample by an external parameter can lead to modulated changes in the concentration $c_i(t)$ of the $i$th species $X_i$. This results in modulated changes of the corresponding absorbance [Fig. 1(a)]. The term ''species'' can be considered as a molecule, a functional group of it, or more general, as a specific state of a molecule (orientation, secondary structure, etc.). However, changes in the thickness $d(t)$ of the sample (e.g., in polymer stretching experiments) or changes of the absorption coefficient $\epsilon_i(\tilde{\nu},t)$ itself (e.g., temperature modulation) can also lead to changes in the time dependent absorbance. Considering the general case of overlapping bands of several species $X_i$, Lambert–Beer's law leads to the periodic time dependent absorbance $A(\tilde{\nu},t)$

$$A(\tilde{\nu},t)=\sum_i A_i(\tilde{\nu},t)=\sum_i \epsilon_i(\tilde{\nu},t)\cdot c_i(t)\cdot d(t)$$

$$=-\log\frac{I_S(\tilde{\nu},t)}{I_R(\tilde{\nu})}, \tag{1}$$

where $I_S(\tilde{\nu},t)$ and $I_R(\tilde{\nu})$ denote the single channel intensities with and without the sample, respectively; the former being time dependent due to external stimulation of the sample $S$, and the latter representing the reference intensity $R$.

The description of the function $A(\tilde{\nu},t)$ in the frequency domain is the subject of the following analysis.

### A. Fourier analysis

According to Fourier's theorem every periodic function of the period $T$ can be expressed as a Fourier series in the form (the noncomplex form is used in all further expressions)

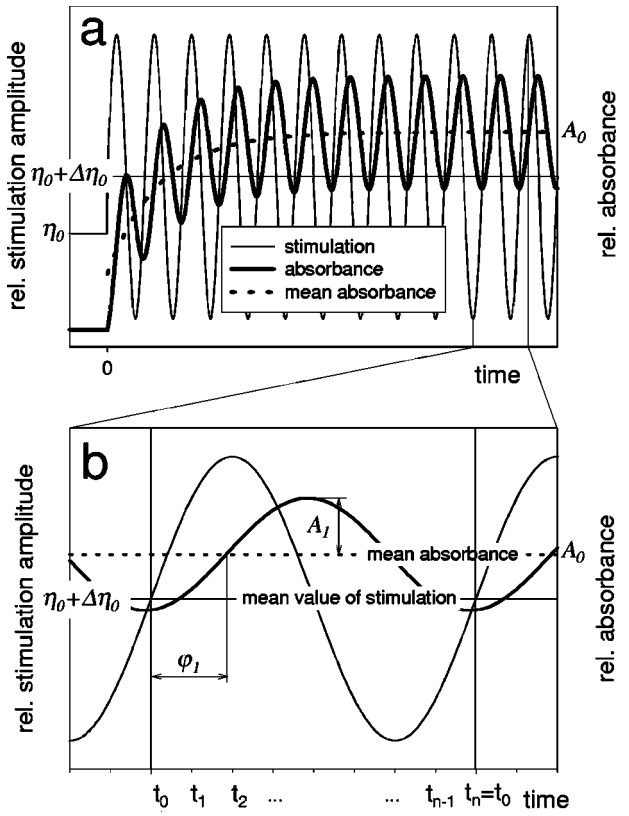


FIG. 1. Periodic stimulation and induced changes in the concentration of an absorbing species. (a) The sinusoidal excitation (e.g., temperature) starts at the time $t=0$ with an additional jump from the initial stimulation value $\eta_0$ to the mean stimulation value $\eta_0+\Delta\eta_0$. After an initial time (in this case approximately five periods) the stationary state is reached. In this state the absorbance varies periodically around a mean value $A_0$. It should be noted that data sampling in modulation spectroscopy always has to be delayed by the time the system is required to reach this stationary state. At low modulation frequencies this can lead to a considerable extension of the measurement time, especially in the step–scan mode. (b) [expanded section of (a)]. In the stationary state the absorbance of the excited species and the stimulation show a phase lag $\varphi_1$, which is characteristic of the kinetics of the stimulated system. $A_1$ is the absorbance modulation amplitude. Calculation was based on first order kinetics, i.e., with a linear system. Consequently, a sinusoidal stimulation cannot produce higher harmonics in the response. In a typical modulation experiment, data acquisition is performed in the stationary state of excitation. The measurement of the $n$ time-resolved spectra takes place at the times $t_i(i=0...n-1)$ and is triggered by the beginning of each stimulation period. The sample points of the $n$ spectra have to fit exactly into the time of one period.

$$f(t)=a_0+\sum_{k=1}^{\infty}\left[a_k\cos(k\omega t)+b_k\sin(k\omega t)\right] \tag{2}$$

with

$$\omega=2\pi f=2\pi/T \text{ and } f=1/T,$$

where $k$ is the frequency multiplier, $k=0$: dc term, $k=1$: fundamental frequency (frequency of stimulation), $k>1$ higher harmonics; $a_0$ is the dc component; $a_k$ is the Fourier coefficient of the cosine component corresponding to frequency $k\omega$; and $b_k$ is the Fourier coefficient of the sine component corresponding to frequency $k\omega$.

The Fourier coefficients $a_0$, $a_k$, and $b_k$ of the periodic function $f(t)$ are given by

$$a_0=\frac{1}{T}\int_0^T f(t)dt,$$

$$a_k=\frac{2}{T}\int_0^T f(t)\cos(k\omega t)dt; \quad k=1,2,\ldots, \tag{3}$$

$$b_k=\frac{2}{T}\int_0^T f(t)\sin(k\omega t)dt; \quad k=1,2,\ldots.$$

$a_k$ and $b_k$ represent the orthogonal components of a vector, which can also be expressed in polar coordinates, i.e., amplitude $c_k$ and phase angle $\varphi_k$.

Setting now

$$a_k=c_k\sin\varphi_k, \quad b_k=c_k\cos\varphi_k \tag{4}$$

and using the trigonometric relation $\sin\alpha\cos\beta+\cos\alpha\sin\beta=\sin(\alpha+\beta)$, the Fourier series, Eq. (2), can be represented as a sine series with an additional phase angle $\varphi_k$

$$f(t)=a_0+\sum_{k=1}^{\infty}\left[c_k\sin\varphi_k\cos(k\omega t)+c_k\cos\varphi_k\sin(k\omega t)\right]$$

$$=a_0+\sum_{k=1}^{\infty}c_k\sin(k\omega t+\varphi_k). \tag{5}$$

The amplitudes $c_k$ and phase lags $\varphi_k$ are given by

$$a_k^2+b_k^2=c_k^2(\sin^2\varphi_k+\cos^2\varphi_k)=c_k^2$$

$$c_k=\sqrt{a_k^2+b_k^2}, \tag{6}$$

$$\sin\varphi_k=\frac{a_k}{c_k}, \quad \cos\varphi_k=\frac{b_k}{c_k}. \tag{7}$$

Now, let us consider a spectroscopic experiment resulting in the overall absorbance $A(\tilde{\nu},t)$ [Eq. (1)] consisting of a stationary (dc) part $A_0(\tilde{\nu})$ and the modulated part $A_m(\tilde{\nu},t)$. If the system consists of $N$ absorbing species we get for the overall absorbance making use of the Fourier series Eq. (2)

$$A(\tilde{\nu},t)=\sum_{i=1}^{N}A_i(\tilde{\nu},t)=\sum_{i=1}^{N}A_{i,0}(\tilde{\nu})$$

$$+\sum_{i=1}^{N}\sum_{k=1}^{\infty}\left[A_{i,k}^{90^\circ}(\tilde{\nu})\cos(k\omega t)\right.$$

$$\left.+A_{i,k}^{0^\circ}(\tilde{\nu})\sin(k\omega t)\right]. \tag{8}$$

For the sake of simplicity, however, the following notations relate only to one species, i.e., the index $i$ and the corresponding sums are omitted.

According to Eq. (3) $A_0(\tilde{\nu})$ denotes the mean absorbance per period (dc term)

$$A_0(\tilde{\nu})=\frac{1}{T}\int_0^T A(\tilde{\nu},t)dt \tag{9}$$

and $A_k^{90^\circ}(\tilde{\nu})$ and $A_k^{0^\circ}(\tilde{\nu})$ the cosine (90°, out of phase) and sine (0°, in phase) Fourier coefficients associated with the angular frequency $k\omega$, respectively. Using Eqs. (3) and (4) $A_k^{90^\circ}(\tilde{\nu})$ and $A_k^{0^\circ}(\tilde{\nu})$ can be written as

$$A_k^{90^\circ}(\tilde{\nu}) = A_k(\tilde{\nu})\sin\varphi_k = \frac{2}{T}\int_0^T A(\tilde{\nu},t)\cos(k\omega t)\,dt,$$
$$k = 1,2,\ldots,$$
$$A_k^{0^\circ}(\tilde{\nu}) = A_k(\tilde{\nu})\cos\varphi_k = \frac{2}{T}\int_0^T A(\tilde{\nu},t)\sin(k\omega t)\,dt, \quad (10)$$
$$k = 1,2,\ldots.$$

According to Eq. (5), $A(\tilde{\nu},t)$ can also be expressed by a sine series with amplitudes $A_k(\tilde{\nu})$ and phase lags $\varphi_k(\tilde{\nu})$

$$A(\tilde{\nu},t) = A_0(\tilde{\nu}) + \sum_{k=1}^{\infty} A_k(\tilde{\nu})\sin[k\omega t + \varphi_k(\tilde{\nu})]. \quad (11)$$

### B. Phase sensitve detection

Phase sensitive detection is a method enabling the evaluation of absolute average amplitudes $A_k(\tilde{\nu})$ and average phase lags $\varphi_k(\tilde{\nu})$ in a spectroscopic modulation experiment. In this respect, it represents an alternative method to Fourier analysis of a periodic function. The expression ''average'' means that the overall absorbance associated with the frequency $k\omega$, $A_k(\tilde{\nu})$, is composed of absorbances $A_{ik}(\tilde{\nu})$ of all species $X_i$ absorbing at wave number $\tilde{\nu}$. Furthermore, each of these components $A_{ik}(\tilde{\nu})$ has its distinct phase lag $\varphi_{ik}(\tilde{\nu})$.

The analytical procedure of a PSD consists of a multiplication of $A(\tilde{\nu},t)$ by, e.g., $\sin(k\omega t+\phi_k^{\mathrm{PSD}})$ followed by a normalized integration over the period $T$. This will introduce an additional parameter, namely the operator controlled phase angle $\phi_k^{\mathrm{PDS}}$ according to Eq. (12)

$$A_k^{\phi_k^{\mathrm{PSD}}}(\tilde{\nu}) = \frac{2}{T}\int_0^T A(\tilde{\nu},t)\sin(k\omega t + \phi_k^{\mathrm{PSD}})\,dt;$$
$$k = 1,2,\ldots. \quad (12)$$

$A_k^{\phi_k^{\mathrm{PSD}}}(\tilde{\nu})$ is referred to as phase-resolved modulation spectrum or phase-resolved absorbance spectrum associated with frequency $k\omega$ ($k=1$ corresponds to the fundamental, i.e., to the frequency of excitation) and PSD phase setting $\phi_k^{\mathrm{PSD}}$. For the special cases $\phi_k^{\mathrm{PSD}}=0^\circ$ and $\phi_k^{\mathrm{PSD}}=90^\circ$, $A_k^{\phi_k^{\mathrm{PSD}}}(\tilde{\nu})$ is equivalent to the in-phase and out-of-phase components of Eq. (10), respectively.

$A_k^{\phi_k^{\mathrm{PSD}}}(\tilde{\nu})$ can be expressed as a linear combination of $A_k^{0^\circ}(\tilde{\nu})$ and $A_k^{90^\circ}(\tilde{\nu})$ using the trigonometric relation $\sin(\alpha+\beta)=\sin\alpha\cos\beta+\cos\alpha\sin\beta$.

$$\begin{aligned} A_k^{\phi_k^{\mathrm{PSD}}}(\tilde{\nu}) &= \frac{2}{T}\int_0^T A(\tilde{\nu},t)[\sin(k\omega t)\cos(\phi_k^{\mathrm{PSD}}) \\ &\quad + \cos(k\omega t)\sin(\phi_k^{\mathrm{PSD}})]\,dt \\ &= \frac{2}{T}\int_0^T A(\tilde{\nu},t)\sin(k\omega t)\,dt\cdot\cos(\phi_k^{\mathrm{PSD}}) \\ &\quad + \frac{2}{T}\int_0^T A(\tilde{\nu},t)\cos(k\omega t)\,dt\cdot\sin(\phi_k^{\mathrm{PSD}}) \\ &= A_k^{0^\circ}(\tilde{\nu})\cos(\phi_k^{\mathrm{PSD}}) + A_k^{90^\circ}(\tilde{\nu})\sin(\phi_k^{\mathrm{PSD}}). \end{aligned} \quad (13)$$

Similar to the transformation done in Eqs. (3)–(5), using Eqs. (10), (13), and $\cos\alpha\cos\beta+\sin\alpha\sin\beta=\cos(\alpha-\beta)$ leads to

$$\begin{aligned} A_k^{\phi_k^{\mathrm{PSD}}}(\tilde{\nu}) &= A_k(\tilde{\nu})\cos(\varphi_k)\cos(\phi_k^{\mathrm{PSD}}) \\ &\quad + A_k(\tilde{\nu})\sin(\varphi_k)\sin(\phi_k^{\mathrm{PSD}}) \\ &= A_k(\tilde{\nu})\cos(\varphi_k - \phi_k^{\mathrm{PSD}}). \end{aligned} \quad (14)$$

As already mentioned, the parameter $\phi_k^{\mathrm{PSD}}$ can be selected by the operator. When $\phi_k^{\mathrm{PSD}}$ is equal to the phase lag of the signal under consideration at a given wave number $\varphi_k(\tilde{\nu})=\phi_k^{\mathrm{PSD}}$, the cosine function of Eq. (14) becomes equal to 1 and the amplitude $A_k^{\phi_k^{\mathrm{PSD}}}(\tilde{\nu})$ becomes maximum and equals the unknown amplitude $A_k(\tilde{\nu})$. Consequently, maximizing of $A_k^{\phi_k^{\mathrm{PSD}}}(\tilde{\nu})$ for a given wave number by variation of $\phi_k^{\mathrm{PSD}}$ results in both the modulation amplitude $A_k(\tilde{\nu})$ and the phase lag $\varphi_k(\tilde{\nu})$ at the wave number $\tilde{\nu}$. On the other hand, for $\phi_k^{\mathrm{PSD}}=\varphi_k(\tilde{\nu})\pm 90^\circ$, the cosine function and thus the amplitude $A_k^{\varphi_k(\tilde{\nu})\pm 90^\circ}(\tilde{\nu})$ becomes zero

$$A_k^{\varphi_k(\tilde{\nu})\pm 90^\circ}(\tilde{\nu}) = 0. \quad (15)$$

Thus the purpose of the PSD in modulation spectroscopy is the evaluation of phase-resolved absorbance spectra $A_k^{\phi_k^{\mathrm{PSD}}}(\tilde{\nu})$ from the time dependent overall absorbance $A(\tilde{\nu},t)$ by means of the algorithm Eq. (12). If the type of the PSD input is not the absorbance $A(\tilde{\nu},t)$, but the spectral intensity or the intensity in the FTIR interferogram, mathematical conversions based on physical law of light absorption have to be applied to the PSD output $A_k^{\phi_k^{\mathrm{PSD}}}(\tilde{\nu})$ as will be discussed in Sec. III.

## III. MODULATED EXCITATION EXPERIMENTS IN FTIR SPECTROSCOPY

### A. Effect of modulated excitation in the intensity spectrum

Modulated excitation of a sample leads to a modulation of the concentration of those parts of the sample that are affected by the external periodic perturbation. As a consequence, the intensity of the IR beam will obtain periodic components with the fundamental frequency $\omega$ and higher harmonics $k\omega$. Up to now we have discussed the effects of the sample modulation on the basis of the absorbance, i.e., a quantity which is directly proportional to the concentration. Optical experiments, however, are always intensity measurements. Absorbance and intensity are related by Lambert–Beer's law Eq. (1). Solving Eq. (1) for the spectral intensity in the sample channel and making use of Eq. (8) neglecting the different species $i$ results in

$$\begin{aligned} I_S(\tilde{\nu},t) &= I_R(\tilde{\nu})\cdot 10^{-A(\tilde{\nu},t)} = I_R(\tilde{\nu})\cdot 10^{-A_0(\tilde{\nu})}\cdot 10^{-A_m(\tilde{\nu},t)} \\ &= I_R(\tilde{\nu})\cdot 10^{-A_0(\tilde{\nu})} \\ &\quad \cdot 10^{-\sum_{k=1}^{\infty}[A_k^{90^\circ}(\tilde{\nu})\cos(k\omega t)+A_k^{0^\circ}(\tilde{\nu})\sin(k\omega t)]}. \end{aligned} \quad (16)$$

The overall absorbance of the sample $A(\tilde{\nu},t)$ is composed of the absorbance of species are not affected by external stimulation $A_0(\tilde{\nu})$ and that of species responding periodically to the modulated external stimulation $A_m(\tilde{\nu},t)$. In many applications $A_m(\tilde{\nu},t) \ll A_0(\tilde{\nu})$.

As a consequence of Eq. (16), there is no linear relation between the experimentally accessible quantity $I_S(\tilde{\nu},t)$ and the desired modulation spectra $A_k^{90°}(\tilde{\nu})$ and $A_k^{0°}(\tilde{\nu})$. In the case of periodically varying sample concentrations $c_i(t)$, the resulting intensity $I_S(\tilde{\nu},t)$ will also be a periodic function that can be expressed by a Fourier series, too [see Eq. (2)]. However, considering Lambert–Beer's law in the form of Eq. (16), the Fourier coefficients of Eq. (3) become much more complicated due to the exponential relation between the intensity $I$ and the time dependent trigonometric functions. According to the Jacobi–Anger theorem,[15] the Fourier coefficients of $I_S(\tilde{\nu},t)$ are modified Bessel functions of the Fourier coefficients of the absorbance $A(t)$. Provided that PSD must be applied to intensity data, and moreover the absorbance $A_m(\tilde{\nu},t)$ does not fulfill the condition $A_m(\tilde{\nu},t) \ll 1$, application of this sophisticated mathematical procedure[15] is a prerequisite to avoiding systematic errors in quantitative analysis introduced by PSD of $I_S(\tilde{\nu},t)$.

The most simple and direct way to eliminate this problem often encountered in spectroscopic data analysis is a conversion of $I_S(\tilde{\nu},t)$ to $\log[I_S(\tilde{\nu},t)]$ according to Eq. (1) before proceeding with PSD. This conversion may be performed by a logarithmic amplifier or by digital methods.

For the sake of simplicity we discuss here only the special case of weak modulated signals, i.e., $A_m(\tilde{\nu},t) \ll 1$, which enables linearization of the exponential in Eq. (16) resulting in

$$10^{-A_m(\tilde{\nu},t)} \cong 1 - A_m(\tilde{\nu},t)\ln(10) + \ldots \forall |A_m(\tilde{\nu},t)| \ll 1. \quad (17)$$

It follows from Eqs. (16) and (17)

$$\begin{aligned} I_S(\tilde{\nu},t) &\cong I_R(\tilde{\nu})10^{-A_0(\tilde{\nu})}\Bigg\{1 - \ln(10) \\ &\quad \cdot \sum_{k=1}^{\infty} [A_k^{90°}(\tilde{\nu})\cos(k\omega t) + A_k^{0°}(\tilde{\nu})\sin(k\omega t)]\Bigg\} \\ &= I_R(\tilde{\nu})10^{-A_0(\tilde{\nu})} \\ &\quad - I_R(\tilde{\nu})10^{-A_0(\tilde{\nu})}\ln(10)\sum_{k=1}^{\infty}[A_k^{90°}(\tilde{\nu})\cos(k\omega t) \\ &\quad + A_k^{0°}(\tilde{\nu})\sin(k\omega t)]. \end{aligned} \quad (18)$$

The first term of Eq. (18) is the dc component denoted by $I_{S,0}(\tilde{\nu})$

$$I_{S,0}(\tilde{\nu}) = I_R(\tilde{\nu}) \cdot 10^{-A_0(\tilde{\nu})}. \quad (19)$$

It can be measured by low-pass filtering of $I_S(\tilde{\nu},t)$, rejecting all time dependent terms of Eq. (18). $I_{S,0}(\tilde{\nu})$ is the time independent intensity spectrum resulting from the mean absorbance $A_0(\tilde{\nu})$ in relation to the reference spectrum $I_R(\tilde{\nu})$.

The Fourier coefficients of the Fourier series Eq. (18) may be determined by a Fourier analysis of the signal, which is equivalent to a PSD with $\phi_k^{\mathrm{PSD}} = 0°$ and $\phi_k^{\mathrm{PSD}} = 90°$. On the other hand, comparing the general form of a Fourier series [Eq. (2)] with Eq. (18), the resulting Fourier amplitudes $I_{S,k}^{90°}(\tilde{\nu})$ and $I_{S,k}^{0°}(\tilde{\nu})$ associated with frequency $k\omega$ are given by

$$\begin{aligned} I_{S,k}^{90°}(\tilde{\nu}) &\cong -I_R(\tilde{\nu}) \cdot 10^{-A_0(\tilde{\nu})} \cdot A_k^{90°}(\tilde{\nu}) \cdot \ln(10) \\ &= -I_{S,0}(\tilde{\nu}) \cdot A_k^{90°}(\tilde{\nu}) \cdot \ln(10), \\ I_{S,k}^{0°}(\tilde{\nu}) &\cong -I_R(\tilde{\nu}) \cdot 10^{-A_0(\tilde{\nu})} \cdot A_k^{0°}(\tilde{\nu}) \cdot \ln(10) \\ &= -I_{S,0}(\tilde{\nu}) \cdot A_k^{0°}(\tilde{\nu}) \cdot \ln(10), \end{aligned} \quad (20)$$

resulting in for the 90° and 0° absorbance components (modulation spectra) $A_k^{90°}(\tilde{\nu})$ and $A_k^{0°}(\tilde{\nu})$, respectively,

$$\begin{aligned} A_k^{90°}(\tilde{\nu}) &\cong -\frac{I_{S,k}^{90°}(\tilde{\nu})}{I_R(\tilde{\nu}) \cdot 10^{-A_0(\tilde{\nu})} \cdot \ln(10)} \\ &= -\frac{I_{S,k}^{90°}(\tilde{\nu})}{I_{S,0}(\tilde{\nu}) \cdot \ln(10)}, \\ A_k^{0°}(\tilde{\nu}) &\cong -\frac{I_{S,k}^{0°}(\tilde{\nu})}{I_R(\tilde{\nu}) \cdot 10^{-A_0(\tilde{\nu})} \cdot \ln(10)} = -\frac{I_{S,k}^{0°}(\tilde{\nu})}{I_{S,0}(\tilde{\nu}) \cdot \ln(10)}. \end{aligned} \quad (21)$$

The dc intensity spectrum $I_{S,0}(\tilde{\nu})$ therefore must be known in order to evaluate the modulation spectra in absolute scale. Furthermore, we want to point out that the intensity modulation spectra $I_{S,k}^{0°}(\tilde{\nu})$ and $I_{S,k}^{90°}(\tilde{\nu})$ may consist of positive and negative values depending on the phase shift $\varphi_k(\tilde{\nu})$ introduced by the system itself.

### B. Effect of modulated excitation in the interferogram

In FTIR spectroscopy the interferogram is the primary signal to be measured. It represents the intensity $I$ as a function of the retardation $\delta$ in the interferometer. In a modulation experiment, the intensity $I_S(\tilde{\nu},t)$ is generally only time dependent at distinct wave number regions $\tilde{\nu}$. The corresponding interferogram $I_S(\delta,t)$, however, will reflect time dependence at all retardations $\delta$. To avoid a mixing of frequencies resulting from the modulation experiment with those originating from the mirror movement of the interferometer, FTIR modulation experiments are performed mainly in the step scan mode.[9,19]

Theoretically, the intensities of the interferogram $I(\delta,t)$ and the single channel spectrum $I_S(\tilde{\nu},t)$ are related by[20]

$$I(\delta,t) = \int_0^{+\infty} I(\tilde{\nu},t)[1 + \cos(2\pi\tilde{\nu}\delta)] \cdot d\tilde{\nu}, \quad (22)$$

where $I(\tilde{\nu},t)$ is determined by the light source as modified by the instrumental characteristics. The influence of the sample (index $S$) is taken into account by introducing Eqs. (16) and (19) into Eq. (22), followed by the application of the linear approximation of Eq. (17)

$$I_S(\delta,t)=\int_0^{+\infty} I_S(\tilde{\nu},t)[1+\cos(2\pi\tilde{\nu}\delta)]\cdot d\tilde{\nu}$$

$$=\int_0^{+\infty} I_{S,0}(\tilde{\nu})\cdot 10^{-\sum_{k=1}^{\infty}[A_k^{90^\circ}(\tilde{\nu})\cos(k\omega t)+A_k^{0^\circ}(\tilde{\nu})\sin(k\omega t)]}\cdot[1+\cos(2\pi\tilde{\nu}\delta)]\cdot d\tilde{\nu}$$

$$\cong\int_0^{+\infty} I_{S,0}(\tilde{\nu})\cdot\left\{1-\ln(10)\cdot\sum_{k=1}^{\infty}[A_k^{90^\circ}(\tilde{\nu})\cdot\cos(k\omega t)+A_k^{0^\circ}(\tilde{\nu})\sin(k\omega t)]\right\}\cdot[1+\cos(2\pi\tilde{\nu}\delta)]\cdot d\tilde{\nu}. \quad (23)$$

Analogous to the wave number domain, the interferogram $I_S(\delta,t)$ is composed of a time dependent and a time independent part. The latter represents the interferogram of the stationary part of the single channel spectrum $I_{S,0}(\tilde{\nu})$ and is given by

$$I_{S,0}(\delta)=\int_0^{+\infty} I_{S,0}(\tilde{\nu})\cdot[1+\cos(2\pi\tilde{\nu}\delta)]\cdot d\tilde{\nu}. \quad (24)$$

Introducing Eq. (24) into the linearized part of Eq. (23) results in

$$I_S(\delta,t)=I_{S,0}(\delta)-\int_0^{+\infty} I_{S,0}(\tilde{\nu})\ln(10)\sum_{k=1}^{\infty}[A_k^{90^\circ}(\tilde{\nu})\cos(k\omega t)+A_k^{0^\circ}(\tilde{\nu})\sin(k\omega t)][1+\cos(2\pi\tilde{\nu}\delta)]\cdot d\tilde{\nu}$$

$$=I_{S,0}(\delta)-\sum_{k=1}^{\infty}\int_0^{+\infty} I_{S,0}(\tilde{\nu})\ln(10)\cdot[A_k^{90^\circ}(\tilde{\nu})\cos(k\omega t)+A_k^{0^\circ}(\tilde{\nu})\sin(k\omega t)]\cdot[1+\cos(2\pi\tilde{\nu}\delta)]\cdot d\tilde{\nu}$$

$$=I_{S,0}(\delta)-\sum_{k=1}^{\infty}\left\{\int_0^{+\infty} I_{S,0}(\tilde{\nu})\ln(10)A_k^{90^\circ}(\tilde{\nu})\cdot[1+\cos(2\pi\tilde{\nu}\delta)]d\tilde{\nu}\cdot\cos(k\omega t)+\int_0^{+\infty} I_{S,0}(\tilde{\nu})\ln(10)A_k^{0^\circ}(\tilde{\nu})\cdot[1+\cos(2\pi\tilde{\nu}\delta)]d\tilde{\nu}\cdot\sin(k\omega t)\right\}. \quad (25)$$

Again we can extract $I_{S,k}^{0^\circ}(\delta)$ and $I_{S,k}^{90^\circ}(\delta)$, which represent the interferograms of the modulation spectra Eq. (18) $I_{S,k}^{0^\circ}(\tilde{\nu})$ and $I_{S,k}^{90^\circ}(\tilde{\nu})$, respectively.

$$I_{S,k}^{90^\circ}(\delta)=-\int_0^{+\infty}\ln(10)A_k^{90^\circ}(\tilde{\nu})I_{S,0}(\tilde{\nu})[1+\cos(2\pi\tilde{\nu}\delta)]d\tilde{\nu}, \quad (26)$$

$$I_{S,k}^{0^\circ}(\delta)=-\int_0^{+\infty}\ln(10)A_k^{0^\circ}(\tilde{\nu})I_{S,0}(\tilde{\nu})[1+\cos(2\pi\tilde{\nu}\delta)]d\tilde{\nu}. \quad (27)$$

Finally we get for the time and retardation dependent intensity $I_S(\delta,t)$ the Fourier series

$$I_S(\delta,t)=I_{S,0}(\delta)+\sum_{k=1}^{\infty}[I_{S,k}^{90^\circ}(\delta)\cos(k\omega t)+I_{S,k}^{0^\circ}(\delta)\sin(k\omega t)]. \quad (28)$$

$I_{S,0}(\delta)$ is the dc component of $I_S(\delta,t)$ and can be measured by low-pass filtering of the signal measured at the retardation $\delta$.

The ''in-phase'' and ''out-of-phase'' interferogram components $I_{S,k}^{0^\circ}(\delta)$ and $I_{S,k}^{90^\circ}(\delta)$ can be evaluated using a PSD lock-in amplifier at frequency $k\omega$ with $\phi_k^{\mathrm{PSD}}=0^\circ$ and $\phi_k^{\mathrm{PSD}}=90^\circ$, respectively. The interferograms are related to the intensity modulation spectra $I_{S,k}^{0^\circ}(\tilde{\nu})$ and $I_{S,k}^{90^\circ}(\tilde{\nu})$, respectively. As stated above, $I_{S,k}^{0^\circ}(\tilde{\nu})$ and $I_{S,k}^{90^\circ}(\tilde{\nu})$ can be negative for certain $\tilde{\nu}$. This has to be considered in the phase correction mode when performing the FFT of $I_{S,k}^{0^\circ,90^\circ}(\delta)$ to obtain $I_{S,k}^{0^\circ,90^\circ}(\tilde{\nu})$.

The 0° and 90° components of the absorbance spectra can be calculated from $I_{S,0}(\tilde{\nu})$ and $I_{S,k}^{0^\circ,90^\circ}(\tilde{\nu})$ using Eq. (21).

Again, the dc component of the interferogram $I_{S,0}(\delta)$ has to be measured in order to evaluate absolute values of the absorbance modulation spectra. Furthermore, the absorbance modulation amplitudes have to be much smaller than 1 for all wave numbers to enable the use of the approximation of Eq. (17). It should be noted, that in case of large modulation amplitudes the Jacobi–Anger theorem[15] has to be applied, otherwise, significant systematic errors must be taken into account upon PSD of the interferogram.

### C. PSD of time-resolved spectra

Both the PSD of the intensity $I(\tilde{\nu},t)$, which is usually performed in modulation experiments with dispersive instruments, and the PSD of the interferogram $I_S(\delta,t)$ with FT instruments are performed on a scalar base, i.e., the detector intensity at a given wave number and retardation, respectively.

In the following we describe a method to determine phase-resolved absorbance spectra, so-called modulation spectra, by sampling time-resolved spectra followed by a vector PSD applied to the whole set of time-resolved spectra.[18] The PSD computation is performed after data sampling has been finished.

All spectra are handled as arrays ($m$ dimensional vectors) containing the intensities or absorbances at $m$ different wave numbers $\tilde{\nu}_i$ at a distinct time $t$

$$\vec{I}(t)=\begin{pmatrix} I(\tilde{\nu}_1,t)\\ I(\tilde{\nu}_2,t)\\ \cdots\\ I(\tilde{\nu}_{m-1},t)\\ I(\tilde{\nu}_m,t)\end{pmatrix},\quad \vec{A}(t)=\begin{pmatrix} A(\tilde{\nu}_1,t)\\ A(\tilde{\nu}_2,t)\\ \cdots\\ A(\tilde{\nu}_{m-1},t)\\ A(\tilde{\nu}_m,t)\end{pmatrix}. \quad (29)$$

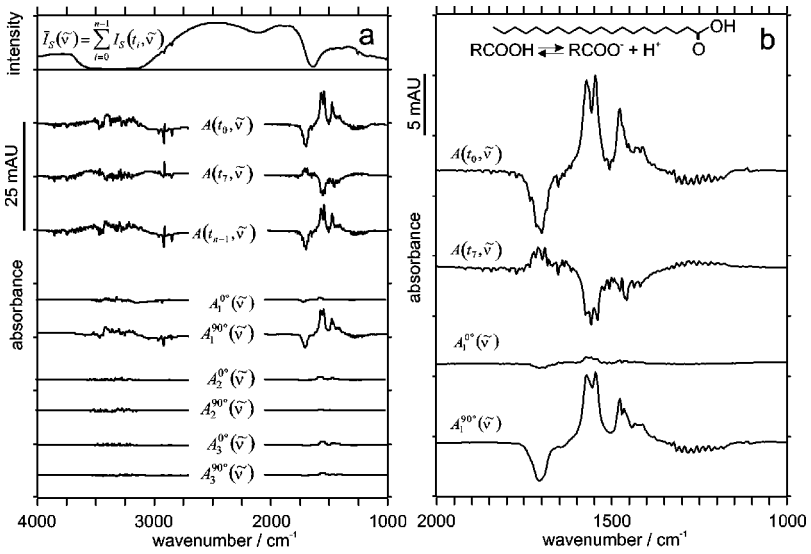


FIG. 2. Time-resolved absorbance spectra and calculated phase-resolved absorbance spectra of an arachidic acid bilayer in a *p*H modulation experiment. The purpose of this experiment was to study the influence of immobilized charges on structural changes in a bilayer model membrane. The arachidic acid bilayer was exposed to a periodic exchange of buffer solutions *p*H 3 and *p*H 7, respectively, with a modulation period of $T=400$ s. An attenuated total reflection (ATR) setup (Ref. 5) was used with parallel polarized incident light at an angle of $\theta=45°$, resulting in $N=25$ active internal reflections. Sixteen sampling point spectra $A(t_i,\tilde{\nu})$ were measured during a period and coadded over ten periods. Data acquisition was started after five initial periods. (a) Mean Intensity spectrum, time-resolved absorbance spectra and phase-resolved modulation spectra. There is very low energy available in the regions of water absorption (3400 and 1640 $cm^{-1}$) as seen in the mean intensity spectrum. This results in a higher noise level of the calculated absorbance spectra $A(t_i,\tilde{\nu})$ ($i=1$, 7, and 15 are shown) in these regions. Periodic protonation and deprotonation of the carboxylic acid groups was induced by the *p*H modulation as can be concluded from a 180° phase shift between the carboxyl stretching vibration $\nu$(COOH) near 1700 $cm^{-1}$ and the stretching vibration $\nu(COO^-)$ near 1560 and 1425 $cm^{-1}$. A phase shift of 180° is manifested by opposite signs of corresponding bands in the modulation spectra $A_1^{0°}(\tilde{\nu})$ and $A_1^{90°}(\tilde{\nu})$, respectively. The in-phase spectrum $A_1^{0°}(\tilde{\nu})$ shows an approximately straight line, whereas the out-of-phase spectrum $A_1^{90°}(\tilde{\nu})$ shows the absorbance of the different states of protonation with a different sign indicating the 180° phase shift. There is only a weak response in the modulated absorption of higher harmonics $A_{2,3}^{0°,90°}(\tilde{\nu})$ indicating that stimulation was close to sinusoidal and that this chemical system exhibits a nearly linear transfer function. (b) Expanded spectral range between 2000 and 1000 $cm^{-1}$. Atmospheric water vapor absorptions (bending vibration) cover the region between 1900 and 1400 $cm^{-1}$. Reduction of these disturbances is generally achieved by purging the spectrometer with a dry gas. However, if strong signal amplification is required remaining incompensations, resulting from the fact that sample and reference spectra have not been measured at the same time, may significantly disturb the line shape of sample absorptions in this region. This is very good recognizable in the time-resolved absorbance spectrum $A(t_{0,7},\tilde{\nu})$ over the whole range of interest. Contrary to time-resolved absorbance spectra, the modulation spectra $A_1^{0°,90°}(\tilde{\nu})$ are completely free of water vapor disturbances although they are the result of PSD calculation from the whole set of time-resolved absorbance spectra. The reason is that the PSD algorithm suppresses all signals that are not labeled by the frequency of excitation. Finally it should be noted, that the sequence of nine weak absorption bands between 1200 and about 1350 $cm^{-1}$ are significant for all-*trans* arrangement of the 18 $CH_2$ groups in the hydrocarbon chain of arachidic acid. The sequence vanishes as soon as one gauche defect is introduced (see e.g., Ref. 3). The phase angle, as concluded from the $A_1^{90°}(\tilde{\nu})$ modulation spectrum, is the same as for the COOH stretching band near 1700 $cm^{-1}$. This enables the unambiguous conclusion, that periodic deprotonation of the COOH group is paralleled by electrostatically induced gauche defects in the hydrocarbon chains. This process is reversible, otherwise PSD would suppress the wagging absorption bands as it did with water vapor absorption.

Data acquisition is started as soon as the periodically stimulated system has reached the stationary state, which is characterized by periodic signal alterations around a constant mean (Fig. 1). This is the case after a time lag corresponding to about three times the longest relaxation time of the system.[3] Now $n$ time resolved intensity spectra $\vec{I}_S(t_i)$ ($i=0\ldots n-1$) of the sample are measured within the stimulation period $T$ at equidistant time intervals $\Delta t=T/n$ as indicated by Eq. (30) and Fig. 1(b)

$$\vec{I}_S(t_i)=\vec{I}_S(t=i\cdot T/n), \quad i=0\ldots n-1. \tag{30}$$

Generally coaddition of the spectra over multiple periods is necessary in order to enhance the signal to noise ratio. Under stationary conditions the intensity spectrum terminating a period ($t=T$) is identical to the intensity spectrum beginning the next period ($t=0$), i.e., $\vec{I}_S(t_n)=\vec{I}_S(t_0)$. Analogous to digital data sampling the intensity spectra $I_S(t_i)$ are referred to as sample point intensity spectra.

A reference spectrum is required in order to convert the acquired intensity spectra into absorbance spectra. Absorbance spectra are aimed for PSD because of their linear dependence of the concentration The arithmetical mean intensity spectrum $\bar{\bar{I}}_S$ may be used for that purpose; the vector elements are given by

$$\bar{\bar{I}}_S(\tilde{\nu})=\frac{1}{n}\sum_{i=0}^{n-1} I_s(t_i,\tilde{\nu}). \tag{31}$$

In this case, the resulting absorbance spectra $\vec{A}(t_i)$ reflect the relative changes of the absorbance during a period. In order to get the physically relevant mean intensity the geometric mean should be evaluated instead of Eq. (31). However, as will be shown below, any reference spectrum may be used in ME spectroscopy to calculate phase-resolved spectra.

An example of a *p*H modulation experiment with an arachidic acid bilayer[21] is shown in Fig. 2(a).

An alternative, even simpler way to achieve absorbance-like spectra, is to simply take the logarithm of the intensity spectrum, which is equivalent to choosing a pseudoreference spectrum $I'_R(\tilde{\nu})=1$. The corresponding absorbance spectrum, their vector elements, and the pseudoreference spectrum are marked by a prime

$$A'(\tilde{\nu},t_i)=-\log\frac{I_S(\tilde{\nu},t_i)}{I'_R(\tilde{\nu})}=-\log I_S(\tilde{\nu},t_i) \tag{32}$$

with $I'_R(\tilde{\nu})=1\forall\tilde{\nu}$. Now we can calculate the Fourier components of $A'(t,\tilde{\nu})$ using the PSD algorithm of Eq. (3) and the Simpson rule [Eq. (33)] for numerical integration

$$\begin{aligned}\int_0^T y(t)dt &\cong \frac{\Delta t}{3}(y_0+4y_1+2y_2+4y_3+\ldots+2y_{n-2}\\ &\quad +4y_{n-1}+y_n)\\ &=\frac{\Delta t}{3}\sum_{i=0}^{n} s_i y_i\end{aligned} \tag{33}$$

with the Simpson coefficients $s_i$ ($n$ must be even).

According to Eq. (9) the constant part (dc term) of $\vec{A}'_0$ results in

$$\begin{aligned}A'_0(\tilde{\nu})&=\frac{1}{T}\int_0^T A'(\tilde{\nu},t)dt\\ &=\frac{\Delta t}{3n\Delta t}\sum_{i=0}^{n} s_i A'(\tilde{\nu},t_i)=\frac{1}{3n}\sum_{i=0}^{n} s_i A'_i(t_i,\tilde{\nu}),\end{aligned} \tag{34}$$

whereas application of Eqs. (10) leads to the 0° and 90° components of the absorbance spectra, i.e., to $\vec{A}'^{\,0^\circ}_k$ and $\vec{A}'^{\,90^\circ}_k$, the in-phase and out-of-phase modulation spectra related to the response with the frequency $k\omega$ (stimulation with $\omega$).

$$\begin{aligned}A'^{\,90^\circ}_k(\tilde{\nu})&=\frac{2}{T}\int_0^T A'(\tilde{\nu},t)\cos(k\omega t)dt\\ &=\frac{2\Delta t}{3n\Delta t}\sum_{i=0}^{n} s_i A'(\tilde{\nu},t_i)\cos\left(k\frac{2\pi}{T}\frac{iT}{n}\right)\\ &=\frac{2}{3n}\sum_{i=0}^{n} s_i A'(\tilde{\nu},t_i)\cos\left(2\pi\frac{ki}{n}\right),\end{aligned} \tag{35}$$

$$\begin{aligned}A'^{\,0^\circ}_k(\tilde{\nu})&=\frac{2}{T}\int_0^T A'(\tilde{\nu},t)\sin(k\omega t)dt\\ &=\frac{2}{3n}\sum_{i=0}^{n} s_i A'(\tilde{\nu},t_i)\sin\left(2\pi\frac{ki}{n}\right).\end{aligned} \tag{36}$$

All our calculations were done with the constant reference $\vec{I}'_R=1$. It will be shown now that only the stationary part of the PSD output $A_0(\tilde{\nu})$ depends on the choice of the reference spectrum, while the modulation spectra resulting from the fundamental and from higher harmonic responses remain unaffected by this choice.

Let $I_R(\tilde{\nu})$ be any real time independent reference spectrum. The mean absorbance spectrum $\vec{A}_0$ related to this reference spectrum is obtained similarly to Eqs. (32) and (34), demonstrating the significance of $I_R(\tilde{\nu})$

$$\begin{aligned}A_0(\tilde{\nu})&=-\log\frac{I_{S,0}(\tilde{\nu})}{I_R(\tilde{\nu})}\\ &=-\log\frac{I_{S,0}(\tilde{\nu})I'_R(\tilde{\nu})}{I'_R(\tilde{\nu})I_R(\tilde{\nu})}=A'_0(\tilde{\nu})-\log\frac{1}{I_R(\tilde{\nu})}\\ &=A'_0(\tilde{\nu})+\log I_R(\tilde{\nu}).\end{aligned} \tag{37}$$

However, as shown by Eq. (38) for $\vec{A}^{0^\circ}_k(\tilde{\nu})$, the modulation spectra $\vec{A}^{0^\circ}_k(\tilde{\nu})$ and $\vec{A}^{90^\circ}_k(\tilde{\nu})$ obtained by the PSD (i.e., calculation of the Fourier coefficients with $k>0$) remain unaffected by the choice of $I_R(\tilde{\nu})$ since the term $\log I_R(\tilde{\nu})\int_0^T\sin(k\omega t)dt=0,\forall k$ vanishes

$$\begin{aligned}A^{0^\circ}_k(\tilde{\nu})&=\frac{2}{T}\int_0^T A(\tilde{\nu},t)\sin(k\omega t)dt\\ &=\frac{2}{T}\int_0^T[A'(\tilde{\nu},t)+\log I_R(\tilde{\nu})]\sin(k\omega t)dt\\ &=\frac{2}{T}\int_0^T A'(\tilde{\nu},t)\sin(k\omega t)dt=A'^{\,0^\circ}_k(\tilde{\nu}).\end{aligned} \tag{38}$$

As a consequence Eqs. (35) and (36) lead to the correct modulation spectra $\vec{A}^{0^\circ}_k$ and $\vec{A}^{90^\circ}_k$ since according to Eq. (38) it follows that $\vec{A}^{0^\circ}_k=\vec{A}'^{\,0^\circ}_k$ and $\vec{A}^{90^\circ}_k=\vec{A}'^{\,90^\circ}_k$. It should be noted that modulation spectra $\vec{A}^{\phi_k^{\mathrm{PSD}}}_k$ may be calculated for any PSD phase angle $\phi_k^{\mathrm{PSD}}$ making use of Eq. (12) and numerical integration Eq. (33)

$$\begin{aligned}A^{\phi_k^{\mathrm{PSD}}}_k(\tilde{\nu})&=\frac{2}{T}\int_0^T A(\tilde{\nu},t)\sin(k\omega t+\phi_k^{\mathrm{PSD}})dt\\ &=\frac{2}{3n}\sum_{i=0}^{n} s_i A(\tilde{\nu},t_i)\sin\left(2\pi\frac{ki}{n}+\phi_k^{\mathrm{PSD}}\right).\end{aligned} \tag{39}$$

The relation between $A^{\phi_k^{\mathrm{PSD}}}_k(\tilde{\nu})$ and the orthogonal modulation spectra $\vec{A}^{0^\circ}_k(\tilde{\nu})$ and $\vec{A}^{90^\circ}_k(\tilde{\nu})$ resulting from Eq. (13) is

$$A^{\phi_k^{\mathrm{PSD}}}_k(\tilde{\nu})=A^{0^\circ}_k(\tilde{\nu})\cos(\phi_k^{\mathrm{PSD}})+A^{90^\circ}_k(\tilde{\nu})\sin(\phi_k^{\mathrm{PSD}}). \tag{40}$$

## IV. EXPERIMENT

### A. A *p*H modulation experiment as an example

Results of a *p*H modulation experiment[3,21] are presented in Fig. 2. The system consisted of an arachidic acid bilayer in an aqueous environment. The bilayer was transferred from the air–water interface to a germanium internal reflection plate by means of the Langmuir–Blodget technique. The external stimulation occurred via periodic exchange of the

aqueous environment using two computer controlled pumps, feeding alternatively solutions of different *p*H.

Figure 2(a) shows on top the mean sample intensity spectrum $\bar{\bar{I}}_S(\tilde{\nu})$ calculated according to Eq. (31). Note the low energy situation in the $H_2O$ stretching (3400 $cm^{-1}$) and bending (1640 $cm^{-1}$) regions. Three time-resolved absorbance spectra are shown in the middle of the figure. The corresponding intensity spectra have been acquired at equidistant time slices of $T/16$, where $T=400$ s denotes the time of a period. Coaddition has been performed in the stationary state. For the sake of common practice, the mean sample intensity spectrum $\bar{I}_S(\tilde{\nu})$ was used as the reference spectrum. Application of Eqs. (35) and (36) lead to the orthogonal modulation spectra shown at the bottom of Fig. 2(a). The main absorption amplitudes are observed in the fundamental response ($k=1,\omega$), however, there are also modulated absorbencies in the fist and second harmonic ($k=2$, 3, meaning $2\omega$ and $3\omega$, respectively). Figure 2(b) shows a scale expanded region of two time-resolved absorbance spectra and the two orthogonal modulation spectra of the fundamental frequency.

Attention should be drawn to the high quality of background compensation reflected by the modulation spectra. Considering, e.g., the time-resolved absorbance spectra $A(t_0,\tilde{\nu})$ and $A(t_7,\tilde{\nu})$ a number of narrow peaks can be observed between 2000 and 1500 $cm^{-1}$, which result from small changes of the water vapor content in the spectrometer during the experiment. The modulation spectra, however, are completely free of these disturbances as shown by $A_1^{0°}(\tilde{\nu})$ and $A_1^{90°}(\tilde{\nu})$. This finding demonstrates the power of modulation spectroscopy in canceling all signals that are not marked by the frequency $\omega$ and/or multiples of it. The noise level of these modulation spectra is found to be below $10^{-5}$ absorbance units. Furthermore, it should be noted that the band sequence observed between 1200 and about 1350 $cm^{-1}$ results from coupled wagging vibrations of the methylene groups in the hydrocarbon chains of arachidic acid. For more details, the reader is referred to Refs. 3 and 21.

### B. Absolute modulation amplitude and phase lag

Absorbance modulation spectra may be expressed as in-phase ($0°,\bar{A}_k^{0°}$) and out-of-phase ($90°,\bar{A}_k^{90°}$) spectra as indicated by Eq. (8). A qualitative correlation analysis of overlapping bands can be performed using the two-dimensional (2D) algorithm introduced by Noda.[22,23] To enhance the quantitative significance of a 2D correlation additional algorithms are described.[16,24]

The most precise method to determine a correlation between two absorbing species, however, is to determine their absolute phase lags in relation to the phase of the periodic stimulation. This can be done by calculation of the absolute absorbance amplitude $\bar{A}_k$ and the corresponding phase spectrum $\bar{\varphi}_k$. With this classical setup of signal analysis, the amplitude and phase spectra quantitatively describe the response of the system in the frequency domain. A correlation of various bands is evident when the phase lag $\varphi_k(\tilde{\nu})$ is identical.[25]

TABLE I. Calculation of the elements of the phase spectrum $\bar{\varphi}_k$ (absolute phase lag) considering the nondetermined range of the arctan function.

| $\varphi_k(\tilde{\nu})$ absolute | $A_k^{0°}(\tilde{\nu})$ | $A_k^{90°}(\tilde{\nu})$ |
|---|---|---|
| $\varphi_k(\tilde{\nu})=\arctan\frac{A_k^{90°}(\tilde{\nu})}{A_k^{0°}(\tilde{\nu})}$ | $A_k^{0°}(\tilde{\nu})\geqslant 0$ | $A_k^{90°}(\tilde{\nu})\geqslant 0$ |
| $\varphi_k(\tilde{\nu})=\arctan\frac{A_k^{90°}(\tilde{\nu})}{A_k^{0°}(\tilde{\nu})}+360°$ | $A_k^{0°}(\tilde{\nu})\geqslant 0$ | $A_k^{90°}(\tilde{\nu})<0$ |
| $\varphi_k(\tilde{\nu})=\arctan\frac{A_k^{90°}(\tilde{\nu})}{A_k^{0°}(\tilde{\nu})}+180°$ | $A_k^{0°}(\tilde{\nu})<0$ | $\forall A_k^{90°}(\tilde{\nu})$ |

With Eq. (6) the elements of the amplitude spectrum $\bar{A}_k$ become

$$A_k(\tilde{\nu})=\sqrt{[A_k^{0°}(\tilde{\nu})]^2+[A_k^{90°}(\tilde{\nu})]^2}. \tag{41}$$

To calculate the absolute phase lag in the range from 0° to 360° one has to consider that the arctan function is not unmistakably determined since $\tan\varphi=\tan(\varphi+180°)$. Therefore one has to use both the sine and the cosine components of the modulation spectra to determine the absolute phase of a modulation absorption band at a given wave number as expressed by Eq. (7).

Table I enables the determination of the absolute phase spectrum $\bar{\varphi}_k$ in the range from 0° to 360°, which is of utmost importance for the determination of the reaction scheme and the kinetic constants of the stimulated system. For details, the reader is referred to Ref. 3.

### C. Phase resolution of overlapping bands

Reliable quantitative IR spectroscopy is often hindered by strongly overlapped absorption bands. Modulation spectroscopy can be used for accurate separation of the components, provided the system may be excited by the variation of any external parameter and moreover the overlapping bands exhibit different phase lags with respect to the stimulation.

In this case the calculation of a set of phase-resolved spectra with different PSD phase settings is very helpful. Let us consider two species $X_\alpha$ and $X_\beta$ with overlapping absorption bands and corresponding phase lags $\alpha$ and $\beta$. It follows from Eq. (15) that there is always a PSD phase setting, resulting in zero absorbance amplitude for a given species. For the species $X_\alpha$ this is the case for $\phi_k^{\mathrm{PSD}}=\alpha\pm 90°$. If, as assumed, the species $X_\beta$ exhibits a different phase lag, its modulation spectrum will not vanish at this PSD phase setting, resulting in a modulation spectrum containing only the absorption band of $X_\beta$. The separation of single components within an overlapping band can thus be achieved on a completely experimental level. By analogous procedure, the absorption band of the species $X_\alpha$ is achieved at PSD phase setting $\phi_k^{\mathrm{PSD}}=\beta\pm 90°$, where the absorption of the species $X_\beta$ is suppressed in the modulation spectrum.

This procedure does not enable the direct determination of the absolute absorbances of the overlapping components, however, in many cases an accurate determination of the band position and its half width is possible. Examples are given in Refs. 3 and 16.

## V. DISCUSSION

The method of vector PSD in spectroscopic modulation experiments can be applied in a wide range of modulation frequencies. Particularly for low frequency modulation ($f < 1$ mHz) PSDs in step–scan mode experiments using lock-in amplifiers become nearly impossible because of very long time constants required for signal-to-noise reduction. For modulation experiments in the low frequency range time-resolved intensity spectra can be acquired in the ordinary rapid scan mode[16] of the FTIR spectrometer. It should be noted, that there is no lower-frequency limit for the application of the algorithm described here.

Experiments with higher modulation frequencies ($1\ \text{Hz} < f < 10\ \text{kHz}$) also benefit from the described algorithm regarding the measurement time and the signal-to-noise ratio.[17] In this frequency range the time-resolved spectra have to be collected in the step–scan mode or in a continuous scan mode.[26]

As the algorithm is based on data sampling of a time-dependent signal, aliasing effects have to be taken into account. There is no possibility of using antaliasing filters. Thus, the time-dependent signal must be oversampled to avoid aliasing artifacts. In the response of the system to a sinusoidal modulated perturbation only frequencies in the range of the modulation frequency and some higher harmonics (nonlinear response) are expected. Thus, the sampling rate of time-resolved spectra must only be about 1 order of magnitude higher than the modulation frequency itself. If the periodic perturbation of the sample is not a simple sinusoidal function, high order harmonics are also to be expected in the linear response of the system. In this case the sampling rate has to be increased in the same amount.

The high-frequency limit of this method is determined by the time resolution of the spectrometer, which generally depends on the conversion rate of the analog-digital-converter (ADC) and/or the time constant of the detector.

In multiple modulation experiments (additional phase modulation in step–scan experiments) the demodulation of the carrier frequency can be performed with a lock-in amplifier before time-resolved intensity spectra are collected. If the carrier frequency is low enough to be sampled by the time-resolved measurement an extension of the algorithm to demodulate both the carrier and the sample modulation should be possible.

Vector PSD as described in this article enables simultaneous detection of the modulation spectra related to the fundamental frequency of stimulation, as well as of higher harmonics up to the limit set by the time resolution of the sampling process. Collection of the same data by conventional methods of PSD of the interferogram[27] would be considerably more time consuming, unless additional lock-in amplifiers and data collection channels could be used. Multifrequency demodulation of the interferogram has recently become possible, however, only with instruments equipped with built in DSP, whereas our method can be used with all types of instruments without additional electronic modifications.

The correct synchronization of data sampling and sample modulation is a prerequisite to use the described PSD algorithm. The procedure for this synchronization is dependent on the modulation experiment, the trigger capabilities, and the mode of time-resolved spectroscopy. In all modes the synchronization of data sampling and sample modulation has to be triggered at the beginning of each modulation period when a coaddition of data sampling is needed, as in most of the cases. For low frequency modulation there is no problem in synchronizing the sample modulation and the data sampling in the rapid scan mode. For higher modulation frequencies, however, sampling of the time-resolved spectra has to be done in the step scan or continuous scan mode. In these modes the correct synchronization can be more difficult.[17]

A further significant advantage of the vector PSD is the ease in determining the absolute values of the absorption modulation amplitude and the phase lag. When using lock-in amplifiers, all additional phase lags and damping properties of the lock-in amplifiers and all other electronic equipment (e.g., low-pass filter) have to be determined to evaluate the absolute amplitudes and phase lags of the absorption with respect to a given stimulus in modulated excitation.

## ACKNOWLEDGMENTS

The authors wish to thank Dr. Thomas Meyer, Büchi Labortechnik AG, CH-9230 Flawil, Switzerland, for writing the fist macros for FTIR modulation spectroscopy. Technical support by Bruker Optik GmbH, D-76275 Ettlingen, Germany (J. Gast, Dr. A. Simon, Dr. J. Gronholz, Dr. K. Rahmelow) is kindly acknowledged.

[1] W. Mäntele, in *Biophysical Techniques in Photosynthesis*, edited by A. Hoff and J. Amesz (Kluwer Academic, Dordrecht, The Netherlands, 1996).
[2] H. Strehlow and W. Knoche, *Fundamentals of Chemical Relaxation* (Verlag Chemie, Weinheim, 1977).
[3] U. P. Fringeli, H. H. Günthard, and D. Baurecht, in *Infrared and Raman Spectroscopy of Biological Materials*, edited by H. U. Gremlich and B. Yan (Marcel Dekker, New York, 2000).
[4] B. O. Seraphim, *Proceedings on the 1st Conference on Modulation Spectroscopy* (North Holland, Amsterdam, 1973).
[5] U. P. Fringeli, in *Internal Reflection Spectroscopy, Theory and Applications*, edited by F. M. Mirabella, Jr. (Marcel Dekker, New York, 1992).
[6] F. Ozanam and J.-N. Chazalviel, Rev. Sci. Instrum. **59**, 242 (1988).
[7] I. Noda, A. E. Dowrey, and C. Marcott, Appl. Spectrosc. **42**, 203 (1988).
[8] R. A. Crocombe and S. V. Compton, *The Design, Performance and Application of a Dynamically-Aligned Step-Scan Interferometer*, FTS/IR Notes **82** (Bio-Rad, Digilab Divison, Cambridge, MA, 1991).
[9] R. A. Palmer, J. L. Chao, R. M. Dittmar, V. G. Gregoriou, and S. E. Plunkett, Appl. Spectrosc. **47**, 1297 (1993).
[10] C. J. Manning and P. R. Griffiths, Appl. Spectrosc. **47**, 1345 (1993).
[11] R. Curbelo, AIP Conf. Proc. **430**, 74 (1998).
[12] C. Marcott, G. M. Story, I. Noda, A. Bibby, and C. J. Manning, AIP Conf. Proc. **430**, 379 (1998).
[13] R. A. Palmer, Spectroscopy (Amsterdam) **8**, 28 (1993).
[14] W. Uhmann, A. Becker, C. Taran, and F. Siebert, Appl. Spectrosc. **45**, 390 (1991).
[15] E. Jahnke and F. Emde, *Tables of Functions with Formulae and Curves* (Dover, New York, 1945).
[16] M. Müller, R. Buchet, and U. P. Fringeli, J. Phys. Chem. **100**, 10810 (1996).
[17] D. Baurecht, and W. Neuhäuser, and U. P. Fringeli AIP Conf. Proc. **430**, 367 (1998).
[18] U. P. Fringeli, International Patent Application, PCT, WO 97/08598 (1997).

[19] R. A. Palmer, C. J. Manning, J. L. Chao, I. Noda, A. E. Dowrey, and C. Marcott, Appl. Spectrosc. **45**, 12 (1991).
[20] P. R. Griffiths, *Chemical Infrared Fourier Transform Spectroscopy* (Wiley-Interscience, New York, 1975).
[21] U. P. Fringeli, in *Encyclopedia of Spectroscopy and Spectrometry*, edited by J. C. Lindon, G. E. Tranter and J. L. Holmes (Academic, Berlin, 2000).
[22] I. Noda, Bull. Am. Phys. Soc. **31**, 520 (1986).
[23] I. Noda, Appl. Spectrosc. **44**, 550 (1990).
[24] S. Ekgasit and H. Ishida, Appl. Spectrosc. **49**, 1243 (1995).
[25] B. O. Budevska, C. J. Manning, and P. R. Griffiths, Appl. Spectrosc. **48**, 1556 (1994).
[26] J. J. Sloan and E. J. Kruus, *Time Resolved Spectroscopy* (Wiley, Chichester, England, 1989).
[27] H. Wang, E. B. Phifer, and R. A. Palmer, Fresenius J. Anal. Chem. **362**, 34 (1998).